FRACTURE PROFILE ANALYSIS OF HEAT TREATED 4340 STEEL*

K. Banerji and E. E. Underwood

Fracture and Fatigue Research Laboratory, Georgia Institute of Technology, Atlanta, GA 30332-0102, USA

ABSTRACT

Hardened and tempered tensile specimens of 4340 steel were fractured at room temperature and the characteristics of the fracture surfaces studied quantitatively through profile analysis. Three parameters were investigated in depth: $R_L(n)$, the lineal roughness parameter; $\nabla\theta\mu$, the mean angular deviation of profile normals from the vertical; and D, the fractal dimension. Pronounced roughness peaks were revealed for specimens tempered between 300° and 400° and at 600°C, and are identified with the well-known embrittlement behavior that occurs in this and similar tempered steels.

KEYWORDS

Quantitative fractography; fracture profile; roughness parameter; fractal dimension; stereology; 4340 steel.

INTRODUCTION

An increased awareness has been shown lately in quantitative fractography and in relating the features of interest in the fracture surface to the conventional SEM photomicrograph. Additional information is frequently sought by means of sections through the fracture surface which permit the details of crack propagation to be observed. These observations of the fracture trace (or profile) are mostly qualitative, or descriptive, in nature. Our objective is concerned more with the quantification of the profile characteristics, thereby enabling the true area of the fracture surface to be determined.

In trying to achieve this objective, two major procedures have evolved. One approach (Bauer, 1981a, 1981b) is essentially nondestructive of the fracture surface in that the elevations at selected points are obtained optically by photogrammetry. The other important method (Underwood, 1981; Coster, 1979; El-Soudani, 1978; Wright, 1983) is destructive of the fracture surface since cuts are made through the fracture surface in order to prepare metallographic sections.

There are several advantages to the latter procedure. One is that the

---

*This work was performed under the auspices of the Metallurgy Program, National Science Foundation, DMR-8204018, Dr. Lance Haworth, Monitor.

underlying microstructure and fracture profile are displayed together in great detail. Moreover, serial sectioning provides a three-dimensional view into the fracture surface region. The incidence of subsurface cracks, voids, particles and boundaries is clearly revealed, allowing the lengths of transgranular and intergranular crack paths to be determined (Underwood, 1979). This sectioning technique also allows the observations of reentrancies in the fracture surface as reproduced by the profile. Since observations are made on the metallographic plane of polish, the well-established equations of stereology (Underwood, 1970a) are available to calculate important quantities in three-dimensional sample space.

However, the basic relationships for nonplanar fracture surfaces are not fully known (El-Soudani, 1974; Chermant, 1983; Underwood, 1981). This stems primarily from the lack of angular randomness of the surface elements. In essence, what we have in the fracture surface is a partially-oriented system of surface elements, and in the fracture profile a partially-oriented system of linear elements (Underwood, 1970b). This situation makes the statistical sampling problem extremely laborious, since extensive angular sampling is required unless symmetry axes or planes exist (Hilliard, 1962; Scriven, 1965).

In addition to the microstructural advantages of the sectioning technique, data obtained from the profile permit the calculation of quantities in the fracture surface. The profile data include the coordinates of points along the trace (at preselected intervals), the angular distribution of the linear segments comprising the trace, the true length of the trace, and the degree of orientation of the linear elements of the profile (Underwood, 1981). In principle, it is then possible to determine the fracture surface characteristics by suitably modified mathematical transform procedures (Hilliard, 1962; Scriven, 1965; Morton, 1967). Thus the importance of the fracture trace and the measurements thereon are apparent. This paper addresses the latter problem and explores the suitability of several parameters that express the characteristics of the fracture profile.

PROFILE PARAMETERS

Seven types of measurements along an irregular planar curve and five possible parameters for characterizing some aspect of the profile have been discussed by Underwood (1984). Here we look at three procedures and the ensuing parameters. The lineal roughness parameter R_L, proposed by Pickens and Gurland (1976), has fundamental significance in these quantitative fractography studies. It is defined by

$$R_L = L_{true}/L' \qquad (1)$$

where L_{true} is the apparent true length of the fracture profile and L' is the projected length of the profile, here, measured parallel to the effective fracture plane.

Another parameter of interest is the concept, due to Mandelbrot (1977), of the fractal dimension D for an irregular planar curve. The basic idea is that the measured length of any irregular curve will depend on the resolution with which it is measured; that is, its measured length will be a function of the size of the measuring unit. As the latter approaches zero, the length of the curve should approach the "true length". Thus, every irregular curve, such as the fracture profile, has an associated "fractal" character which can be expressed quantitatively through the parameter D . The governing equation is

$$L(\eta) = L_o \eta^{1-D} \qquad (2)$$

where $L(\eta)$ is the length estimate and η is the length of the resolution step (or "mean segment length"). D is equal to or greater than one, depending on the irregularity of the curve and the size of η with respect to the actual local profile irregularities. Thus, according to Eq. (2), a log-log plot of $L(\eta)$ vs. η should yield a straight line, the slope of which equals (1-D). Many workers have reported on the results of their fractal analyses and have speculated on the relationship of D to the configuration of the curve (Coster, 1979; Airoldi, 1982; Flook, 1982; Kaye, 1978). A modified form of Eq. (2) is used in this paper, viz.:

$$R_L(\eta) = \frac{L_o}{L'} \eta^{-(D-1)} \qquad (3)$$

where the roughness parameter is a function of η. L_o/L' is a constant, and $-(D-1)$ is the slope of the log-log plot of $R_L(\eta)$ vs. η.

A third procedure was queried as to its suitability for characterizing an irregular curve. The method is based on the angular distribution of segment normals along the profile. The parameter chosen is the mean angular deviation of the segment normals from the vertical, $\bar{\nabla\theta}_\mu$. The values vary, of course, depending on the magnitude of the mean segment length and the complexity of the profile.

EXPERIMENTAL PROCEDURES

Material and Sample Preparation

High quality commercial grade 4340 steel rod with nominal composition given in Table I was used.

TABLE 1 Nominal Composition of 4340 Alloy Steel (wt.%)

C	Ni	Cr	Mn	Mo	Si	S	P	Fe
0.41	1.71	0.79	0.75	0.24	0.25	0.011	0.005	Balance

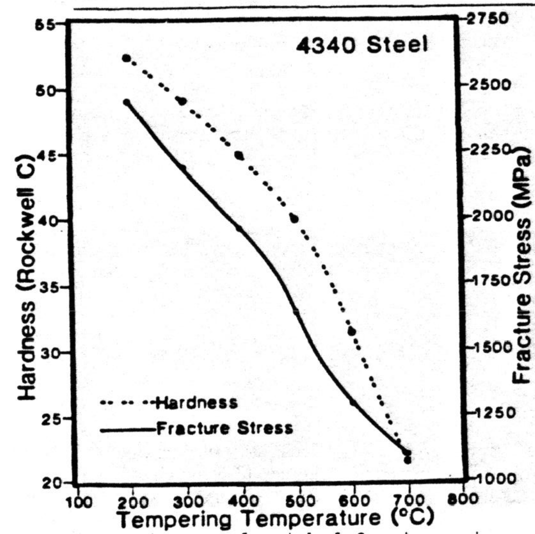

Fig. 1. Hardness and notched fracture stress of 4340 steel vs. tempering temperature.

The material was hardened, then tempered for 1.5 hours at a temperature of 200°C, 300°C, 400°C, 500°C, 600°C or 700°C and oil quenched. Standard 12.83 mm (0.505 inch) diameter ASTM tensile specimens were machined with a 60° circumferential notch of depth 0.864 mm (0.034 inch) in order to insure that the fracture surfaces were effectively perpendicular to the stress axis. The specimens were fractured at room temperature under tension. The fracture stresses and Rockwell-C hardnesses are recorded in Figure 1 vs. tempering temperature.

The fracture surfaces were cut from the broken specimens for both SEM and metallographic investigation. The first cut was made below the fracture surface on a transverse plane perpendicular to the specimen axis so as to provide an accurate orientation reference plane. Representative SEM photographs of the fracture surfaces were taken at various magnifications in the central portion of the fracture in order to record the essential features. The fracture surfaces were then coated with a layer of nickel for edge retention, sectioned vertically and mounted metallographically.

Data Acquisition

After polishing and etching, the six profiles were digitized using a Zeiss Videoplan Image Analysis System. Measurements were obtained directly from the metallographic samples using a drawing tube and digitizing tablet. The central region of each profile was selected for digitizing, keeping the horizontal length constant at about 5 mm.

X-Y coordinates were output at about every 0.7 micron along the actual profile, then transmitted to the Georgia Tech Mainframe Cyber computer for analysis. The mean segment length along the profile was varied by successively considering every second, third, etc. point from the original digitized profile (Banerji, 1983). In this way ten mean segment lengths were obtained between about 0.7 micron and 123 microns.

RESULTS AND DISCUSSION

The variation of fracture strength and hardness as a function of tempering temperature (Fig. 1) is quite typical. Observation of the fracture surfaces at low magnification revealed crack propagation from one side of the specimen to the other, with a deep shear lip in some cases. The vertical sections were cut perpendicular to the crack propagation direction, avoiding the shear lip region.

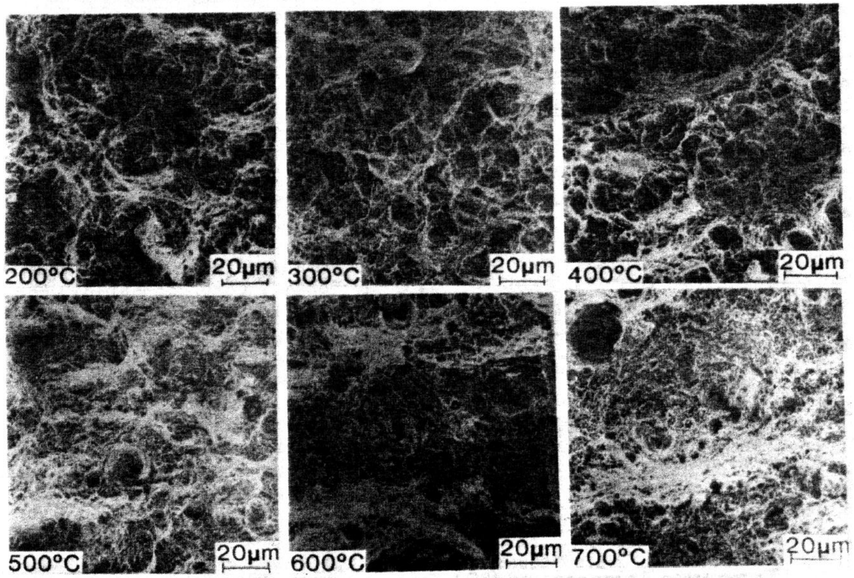

Fig. 2. SEM fractographs of notched 4340 steels tempered at indicated temperatures and fractured under tension at room temperature.

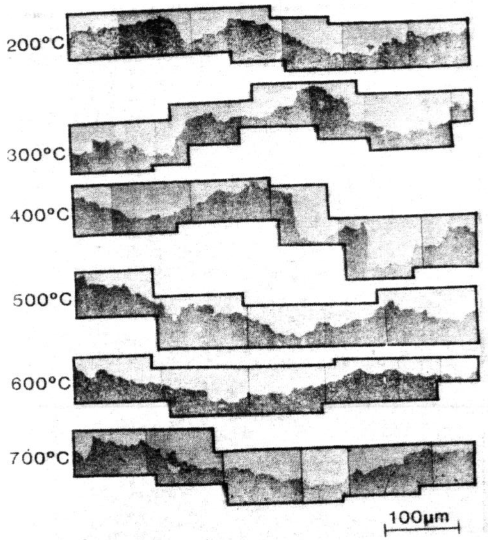

Fig. 3. Examples of fracture profiles in 4340 steels tempered at indicated temperatures.

Optical micrographs of the tempered microstructures show the typical variation from a martensitic to a spheroidal carbide structure. The prior austenitic intercept grain size was determined to be 10.7 µm. Figure 2 shows representative SEM fracture pictures taken from the central portion of the specimen. They will be discussed later. Figure 3 records portions of the six profiles that were analyzed quantitatively. Qualitatively, it appears that these profiles are quite similar and undergo only gradual changes, if any. However, quantitative results obtained with the profile parameters demonstrate significant differences.

Figure 4 is a plot of R_L vs. mean segment length, η, for all six profiles. Each curve shares the same characteristics; that is, there is a rapidly decreasing region (η small), and a relatively flat portion (η large), (Banerji, 1983). Physically, this behavior implies that when the "measuring yardstick" (the mean segment length) is small compared with the scale of local profile roughness, it interacts more with the irregularities. As the mean segment length gets larger, it interacts less with the finer features, and the measured profile length decreases rapidly. At larger and larger values of the mean segment length, it "rides over" the local irregularities and the measured profile length is not greatly affected by variations in η. Thus, these two distinct regions seem appropriate for isolating effects of microroughness at a local level from effects related to long-range undulations in the profile.

In an effort to devise an objective procedure for separating the two regions, log-log plots were made with the same two parameters (see Fig. 5). A sigmoidal shape is obtained for all profiles instead of a linear curve as predicted by Eq. 3. Although the overall slopes computed by linear regression show a correlation coefficient better than -0.99, it is obvious that the local slopes go through a maximum at the inflection point of each curve. The location of the maximum slope is the logical dividing line between the two regions. This separation is important when the profile consists of local roughness superimposed on smooth background undulations.

Three parameters were selected to delineate the effect of tempering temperature on the profile "roughness". They are (i) the overall fractal dimension, $\bar{D}$; (ii) the lineal roughness parameter, $R_L(\eta)$; and (iii) the mean angular deviation of the trace normals from the profile perpendicular, $V\theta\mu$. Figures 6, 7 and 8 portray the variation of each of these parameters with tempering temperature. In addition, both Fig. 7 and 8 show the effect of variations in the mean segment length.

There are striking similarities among the three plots. First, the parameters

Fig. 4. R_L v. η.(↓)

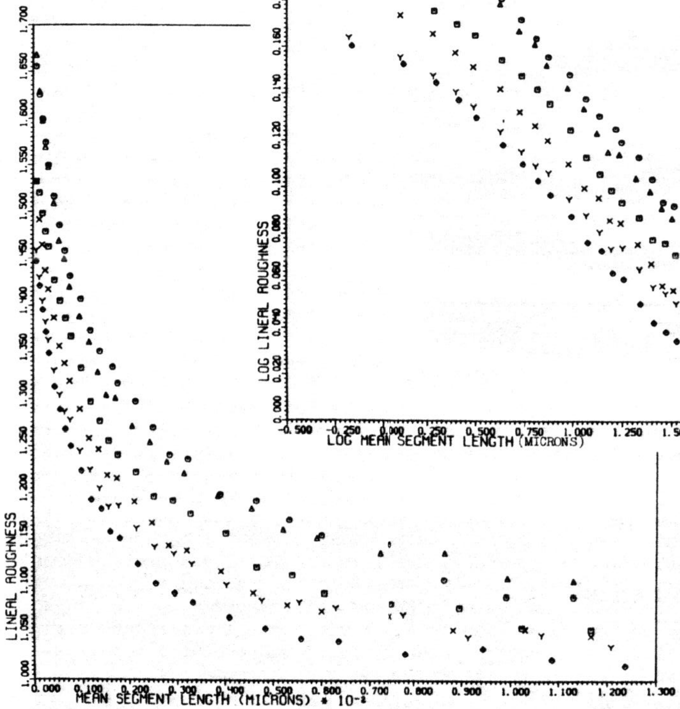

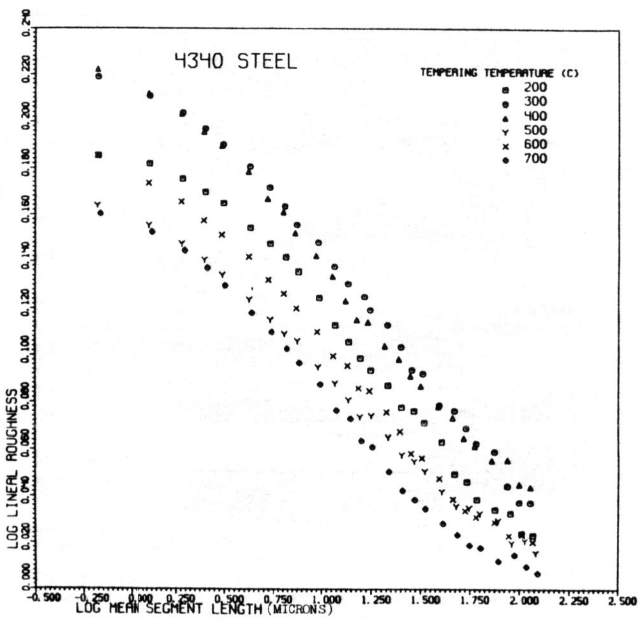

Fig. 5. log R_L vs. log η. (↑)

peak between 300 and 400°C and at 600°C; second, there is a relative minimum at 500°C; and third, the parameter values in Figs. 7 and 8 increase with decreasing η (as indicated by Eq. 3). The three parameters originate from different characteristics of the profile, yet they seem to be related. However, the exact analytical relationships are not obvious at present.

The variation of these parameters with tempering temperature are consistent with the fracture mechanisms operative in 4340 and similar HSLA steels. The two peaks correspond to the transformation of retained austenite at 300 and 600°C. At the lower temperature, the austenite transforms to a tough, plate-like lower bainite. Moreover, distinct tear ridges were observed in the specimens tempered at 300 and 400°C. If tempered at 600°C, a brittle pearlite structure is formed. The crack propagates preferentially either through the pearlite boundaries or the ferrite-cementite interfaces. At both temperatures the increased roughness parameters can be attributed to the type of microstructure obtained on tempering and its influence on the fracture path.

The parameter minima at 500°C are probably associated with temper embrittlement (Tetelman, 1967), whereby the fracture proceeds by intergranular dimpled

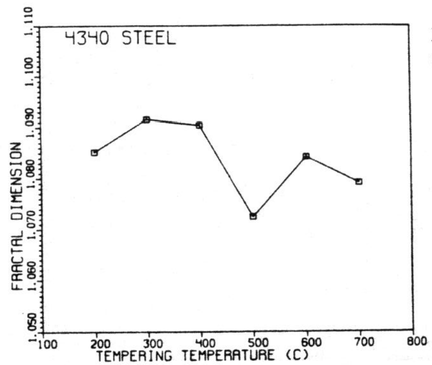

Fig. 6. Variation of mean fractal dimension $\overline{D}$ with tempering temperature.

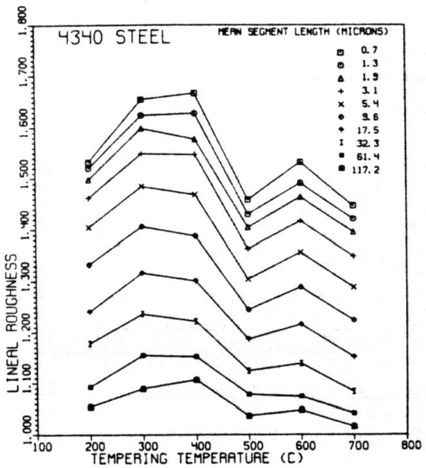

Fig. 7. Variation of R_L vs. tempering temperature for different values of η.

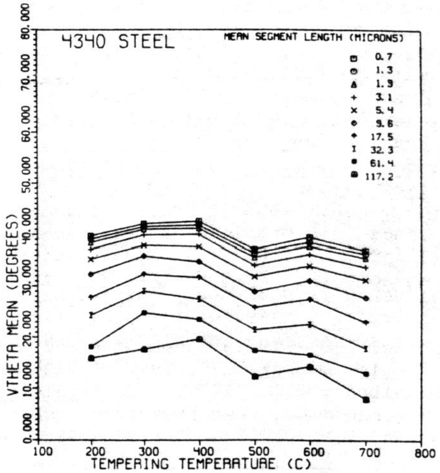

Fig. 8. Variation of $V\theta\mu$ with tempering temperature for different values of η.

rupture and consequently the roughness is low. The two relatively low parameter values at 200 and 700°C can also be traced to the microstructures obtained upon tempering. At 200°C the fracture path is probably along martensite lath boundaries, while at 700°C, fracture is due to transgranular dimple formation associated with fine spheroidal carbides.

CONCLUSIONS

The fracture profiles of six fractured 4340 steel tensile specimens were studied in terms of the roughness parameter, R_L; the mean fractal dimension, $\overline{D}$; and the mean angular deviation of profile normals from the vertical, $V\theta\mu$ Although each parameter measures a different attribute of the profile, qualitatively similar trends are found for each vs. tempering temperature. A pronounced minimum in the roughness curves is seen at 500°C and is associated with temper embrittlement. Roughness peaks at 300-400°C and 600°C correspond to the rough, jagged crack paths induced by the corresponding tempered microstructures.

REFERENCES

Airoldi, G. (1982). Quantitative fracture surface profile analysis in environmental fatigue tests. In K.L. Maurer and F.E. Matzer (Eds.), Procs. 4th European Conf. on Fracture (Leoben, Austria, 22-24, Sept. 1982). 599-606.

Banerji, K. and E.E. Underwood (1983). Quantitative analysis of fractographic features in a 4340 steel. In M. Kališnik (Ed.), Procs. of the 6th Int. Cong. for Stereology (Gainesville, FL, USA, 9-14, Oct. 1983). To be published.

Bauer, B. and H.E. Exner (1981a). Quantification and reconstruction of spatial objects and surfaces by computer aided stereometry. In M. Kališnik (Ed.), Procs. 3rd Eur. Symp. for Stereology (Ljubljana, Yugoslavia), Vol. 3, (Suppl. 7) 255-262.

Bauer, B. and A. Haller (1981b). Determining the three dimensional geometry of fracture surfaces. Practical Metallography, 18, 327-341.

Chermant, J.-L. and M. Coster (1983). Recent developments in quantitative fractography. Int. Metals Reviews, 28, 228-250.

Coster, M., J.-L. Chermant and P. Dujardin (1979). Quantitative fractography with digitalization table. Proc. 5th Int. Cong. for Stereology (Salzburg, Austria, Sept. 1979). 364-372.

El-Soudani, S.M. (1974). Theoretical basis for the quantitative analysis of fracture surfaces. Metallography, 7, 271-311.

El-Soudani, S.M. (1978). Profilometric analysis of fractures. Metallography, 11, 247-336.

Flook, A.G. (1982). Fractal dimensions: Their evaluation and their significance in stereological measurements. Acta Stereologica, 1, 79-87.

Hilliard, J.E. (1962). Specification and measurement of microstructural anisotropy. Trans. AIME, 224, 1201-1211.

Kaye, B.H. (1978). Specification of the ruggedness and/or texture of a fine particle profile by its fractal dimension. Powder Technology, 21, 1.

Leslie, W.C. (1981). Heat-treated steels. In The Physical Metallurgy of Steels, McGraw-Hill. Chap. 7, 236-242.

Mandelbrot, B.B. (1977). In Fractals, Form, Chance and Dimension. W. H. Freeman & Co., San Francisco. Chap. II, 42.

Morton, V.M. (1967). The distribution of angular distributions of planes in space. Proc. Roy. Soc., A302, 51-68.

Pickens, J.R. and J. Gurland (1976). Metallographic characterization of fracture surface profiles on sectioning planes. In E. E. Underwood, et al. (Eds.), Procs. 4th Int. Cong. for Stereology (Gaithersburg, Md, USA, Sept. 1975), 269-272.

Scriven, R.A. and H.D. Williams (1965). The derivations of angular distributions of planes by sectioning methods. Trans. AIME, 223, 1593-1602.

Tetelman, A.S. and A.J. McEvily, Jr. (1967). Fracture of steel. In Fracture of Structural Materials, John Wiley. Chap. 10, 493-548.

Underwood, E.E. (1970a). Statistically Exact Expressions. In Quantitative Stereology, Addison-Wesley. Chap. 2, 23-47.

Underwood, E.E. (1970b). Oriented structures. In Quantitative Stereology, Addison-Wesley, Chap. 3., 48-75.

Underwood, E.E. and E.A. Starke, Jr. (1979). Quantitative stereological methods for analyzing important microstructural features in fatigue of metals and alloys. In J. T. Fong (Ed.), Fatigue Mechanisms, ASTM STP 675, 633-682.

Underwood, E.E. and S.B. Chakrabortty (1981). Quantitative fractography of a fatigued Ti-28V alloy. In L.N. Gilbertson and R.D. Zipp (Eds.), Fractography and Materials Science, ASTM STP 733, 337-354.

Underwood, E.E. (1984). Practical Solutions to Stereological Problems. In J.L. McCall and J.H. Steele (Eds.), Practical Applications of Quantitative Metallography, ASTM STP 839. To be published.

Wright, K. and B. Karlsson (1983). Topographic quantification of non-planar localized surfaces. J. of Microscopy, 130, Pt. 1, 37-51.